Supporting Information

Morphology Evolution of Single-Crystalline Hematite Nanocrystals: Magnetically Recoverable Nanocatalyst for Enhanced Facets-Driven Photoredox Activity

*Astam K. Patra,[a] Sudipta K. Kundu,[b] Asim Bhaumik,[b] Dukjoon Kim[a]**

[a] School of Chemical Engineering, Sungkyunkwan University, Suwon, Kyunggi, 440-746 (Republic of Korea), E-mail: djkim@skku.edu.

[b] Department of Materials Science, Indian Association for the Cultivation of Science, 2A & B, Raja S.C. Mullick Road, Jadavpur, Kolkata-700032 (India), E-mail: msab@iacs.res.in.

Table of Content

Table S1. The details of sample name, hydrothermal temperature and reaction duration of the syntheses condition with the corresponding morphology and phase of the materials.

Sample Name	Hydrothermal Temperature	Hydrothermal Duration (hrs)	Morphology[a]	Phase of the Material[b]
S25-NP	298 K	36	Nanoparticle (NP)	Goethite
S75-NR	348 K	36	Nanorod (NR)	Goethite
S120-NR	393 K	36	Nanorod (NR)	Hematite
S150-NC	423 K	36	Nanocuboid (NC)	Hematite
S180-IS	453 K	36	Irregular shape (IS)	Hematite
S180-BTD	453 K	72	Bitruncated-dodecahedron (BTD)	Hematite
S200-BTEO	473 K	36	Bitruncated-elongated octahedron (BTEO)	Hematite
S200-BTO	473K	72	Bitruncated-octahedron (BTO)	Hematite

[a] Analysis by FESEM, [b] Analysis by PXRD

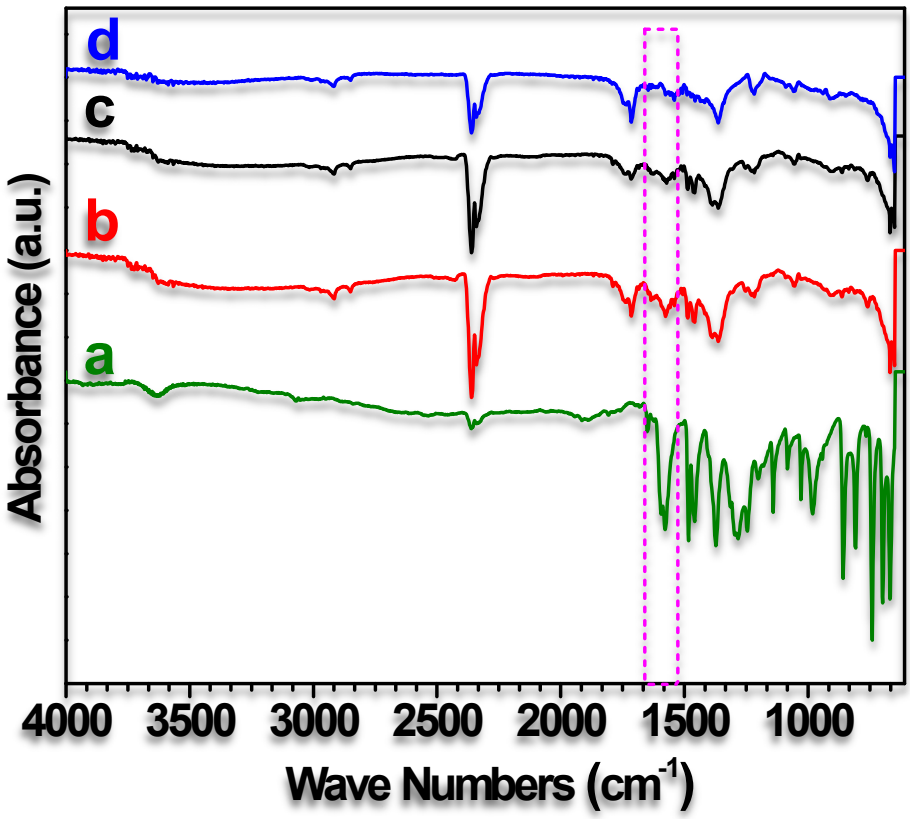

Fig. S1: The FT IR spectra of (a) sodium salicylate, (b) S200-BTO after washing with water and ethanol, (c) S200-BTO after acid-ethanol extraction, and (d) S200-BTO after calcined at 773 K for 6 hrs.

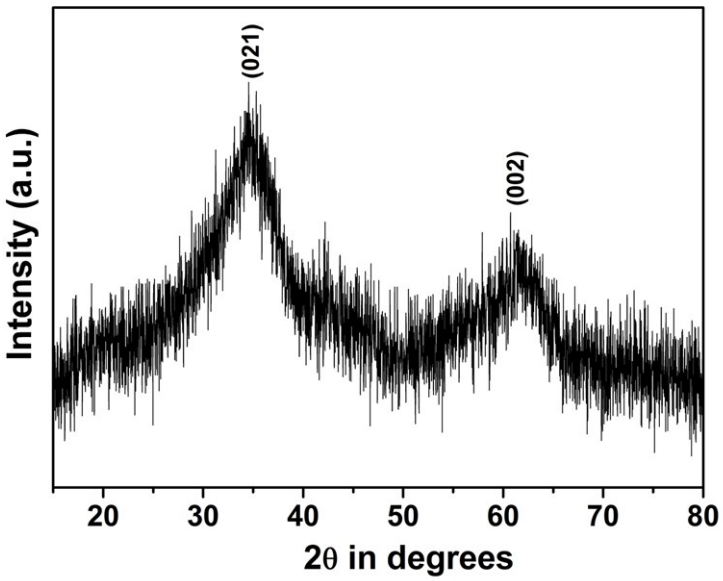

Fig. S2: Wide angle XRD of S25-NP nanoparticles.

Table S2. Comparison of XRD relative intensities from different planes of hematite nanocrystals with different morphologies.

Morphology	$I_{(012)}/ I_{(104)}$	$I_{(012)}/ I_{(110)}$	$I_{(104)}/ I_{(110)}$	Result
JCPDS PDF no 01-084-0308	0.325	0.450	1.383	
Nanorod	0.303	0.373	1.227	$I_{(110)}$ increase
Nanocube	0.332	0.405	1.220	$I_{(012)}$ increase
Bitruncated-dodecahedron	0.275	0.364	1.322	$I_{(104)}$ increase
Bitruncated-elongated octahedron	0.332	0.402	1.211	$I_{(012)}$ and $I_{(110)}$ increase
Bitruncated-octahedron	0.342	0.410	1.199	$I_{(012)}$ and $I_{(110)}$ increase

Table S3. Intensity ratio of E_g to A_{1g} vibration Raman modes of hematite nanocrystals with different exposed facets.

Sample	Morphology	E_g/A_{1g}
S120-NR (a)	**Nanorod**	**1.75**
S150-NC (b)	**Nanocuboid**	**1.52**
S180-BTD (d)	**Bitruncated-dodecahedron**	**1.67**
S200-BTEO (e)	**Bitruncated-elongated octahedron**	**1.89**
S200-BTO (f)	**Bitruncated-octahedron**	**1.92**

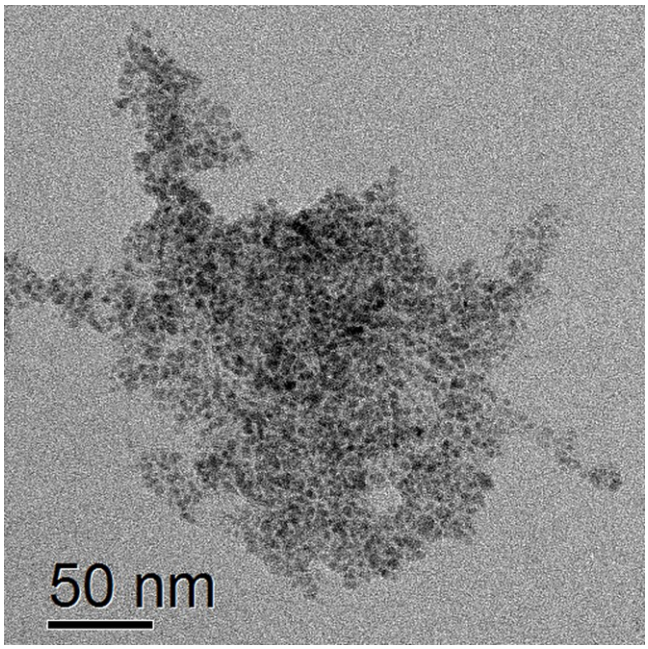

Fig. S3: TEM image of goethite nanoparticles was obtained at room temperature.

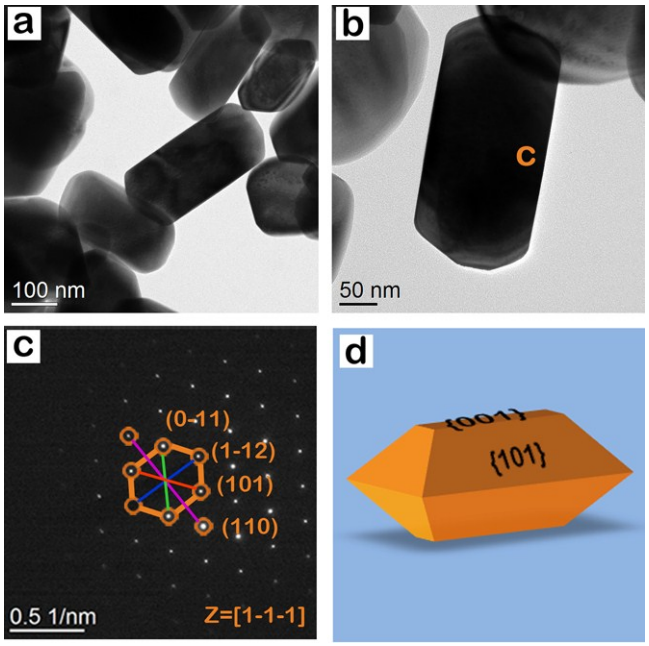

Fig. S4: a) TEM image of bitruncated-elongated octahedron-shaped hematite nanocrystal, b) TEM image single bitruncated-elongated octahedron-shaped hematite nanocrystal, c) corresponding SAED pattern the mark area c of the Fig. S4b with indexing (110), (101) (1-12) and (0-11) lattice spot. The measured angle between (101) and (0-11) is 110^{o}, and between (101) and (1-12) is 55^{o} for both diffraction patterns, d) Geometrical model of the bitruncated-elongated octahedron -shaped hematite nanocrystal with exposed facets.

Fig. S5 [Patra *et al*]

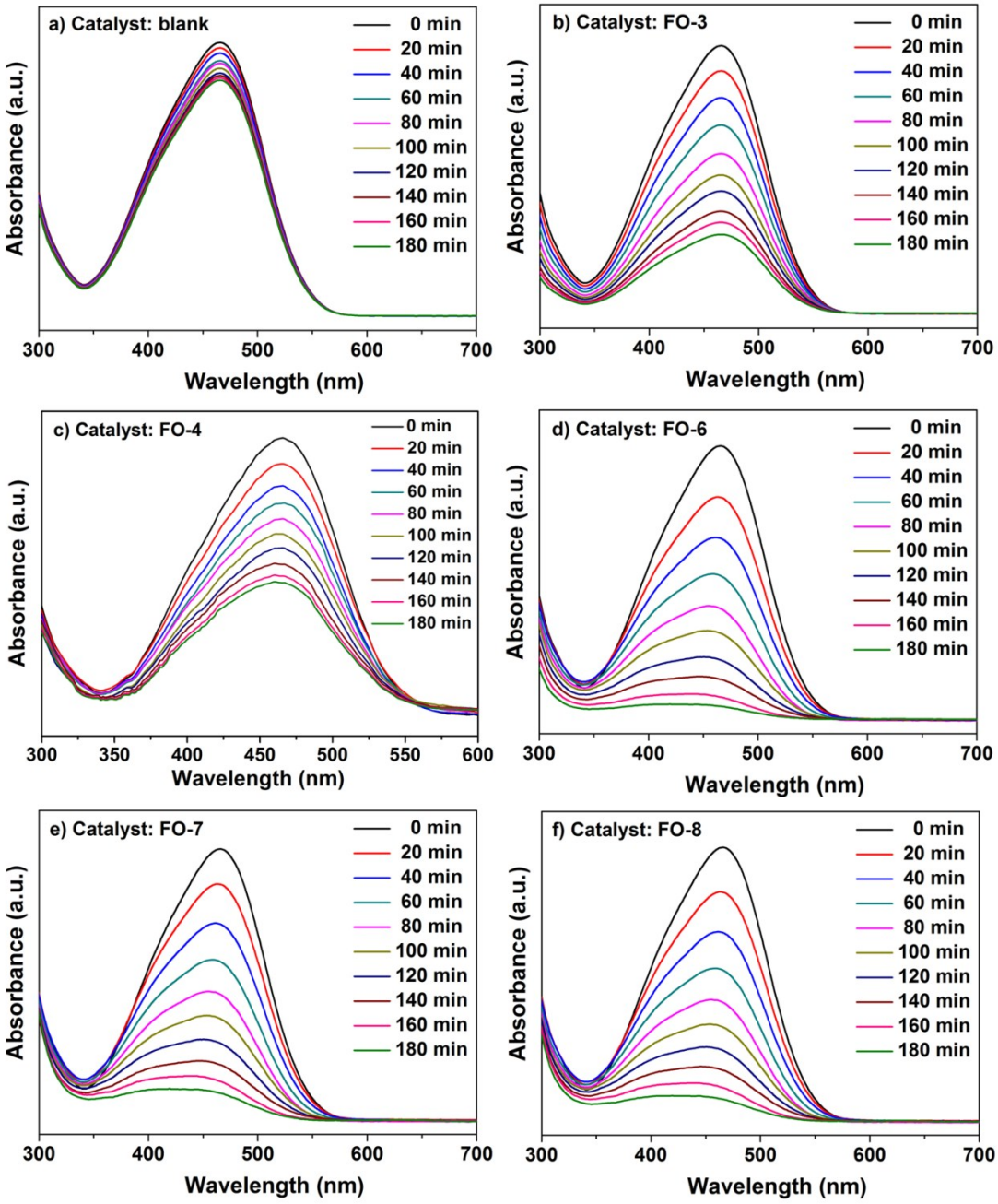

Fig. S5: UV-vis spectral changes of methyl orange aqueous solutions as a function of irradiation time in the presence of hematite photocatalyst and H_2O_2 additive. Reaction conditions: 50 ml 0.02 mM MO dye solution + 10 mg catalyst +0.5 ml H_2O_2 (30 wt %) + white light. a) blank, b) nanorod, c) nanocuboidal, d) bitruncated-dodecahedron, e) Bitruncated-elongated octahedron, f) Bitruncated- octahedron-shaped hematite nanocrystals.

Table S4: Identification of major intermidiates product from the MO degradation reaction by LC-MS (nagative ion mode ESI-MS).

Retention Time (min)	Peak	m/z	Formula
1.79	**A**	**304**	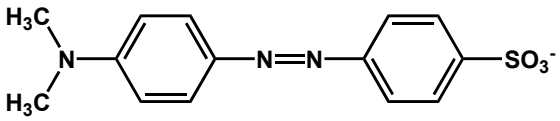
1.38	**B**	**290**	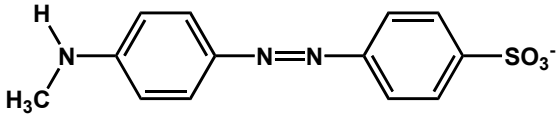
1.06	**C**	**97**	**$[HSO_4]^-$**

Fig. S6 [Patra *et al*]

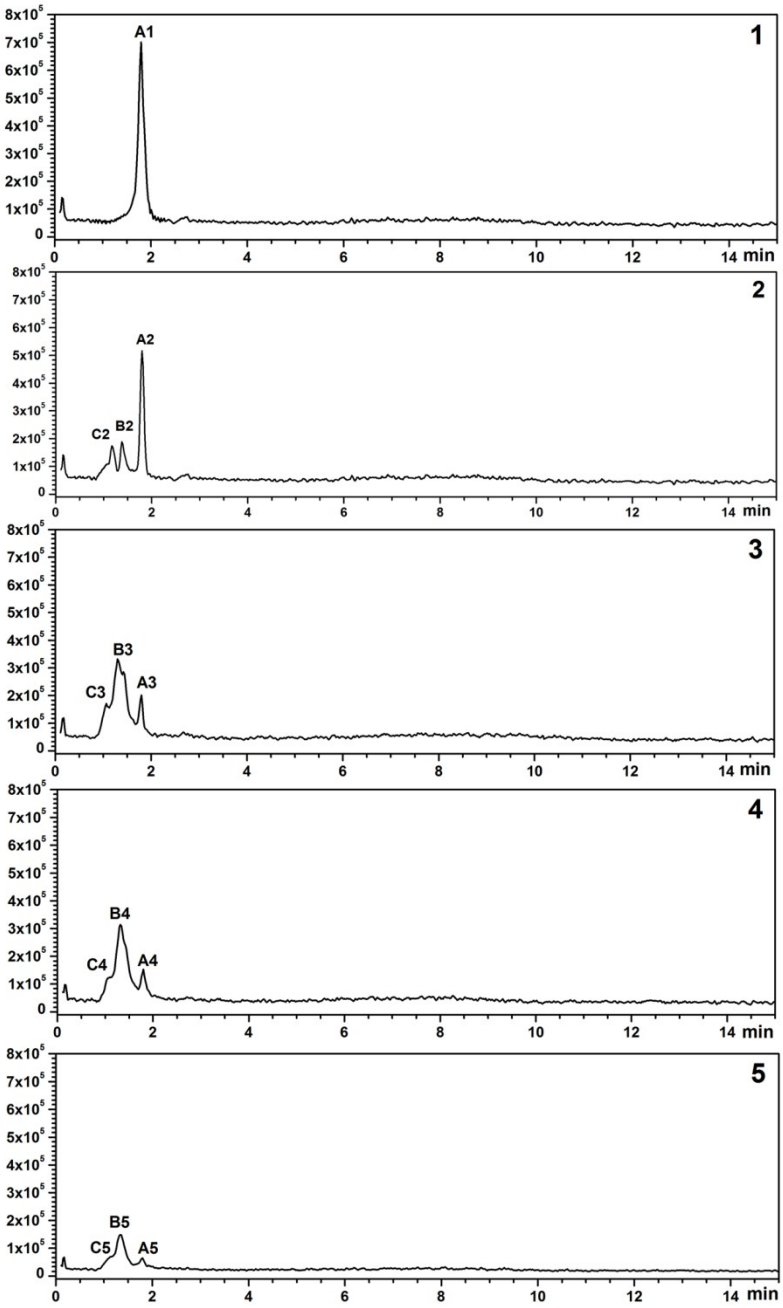

Fig. S6: Total ion chromatography of MO with different intermediate products 1) 0 min, 2) 20 min, 3) 60 min, 4) 80 min, 5) 120 min.

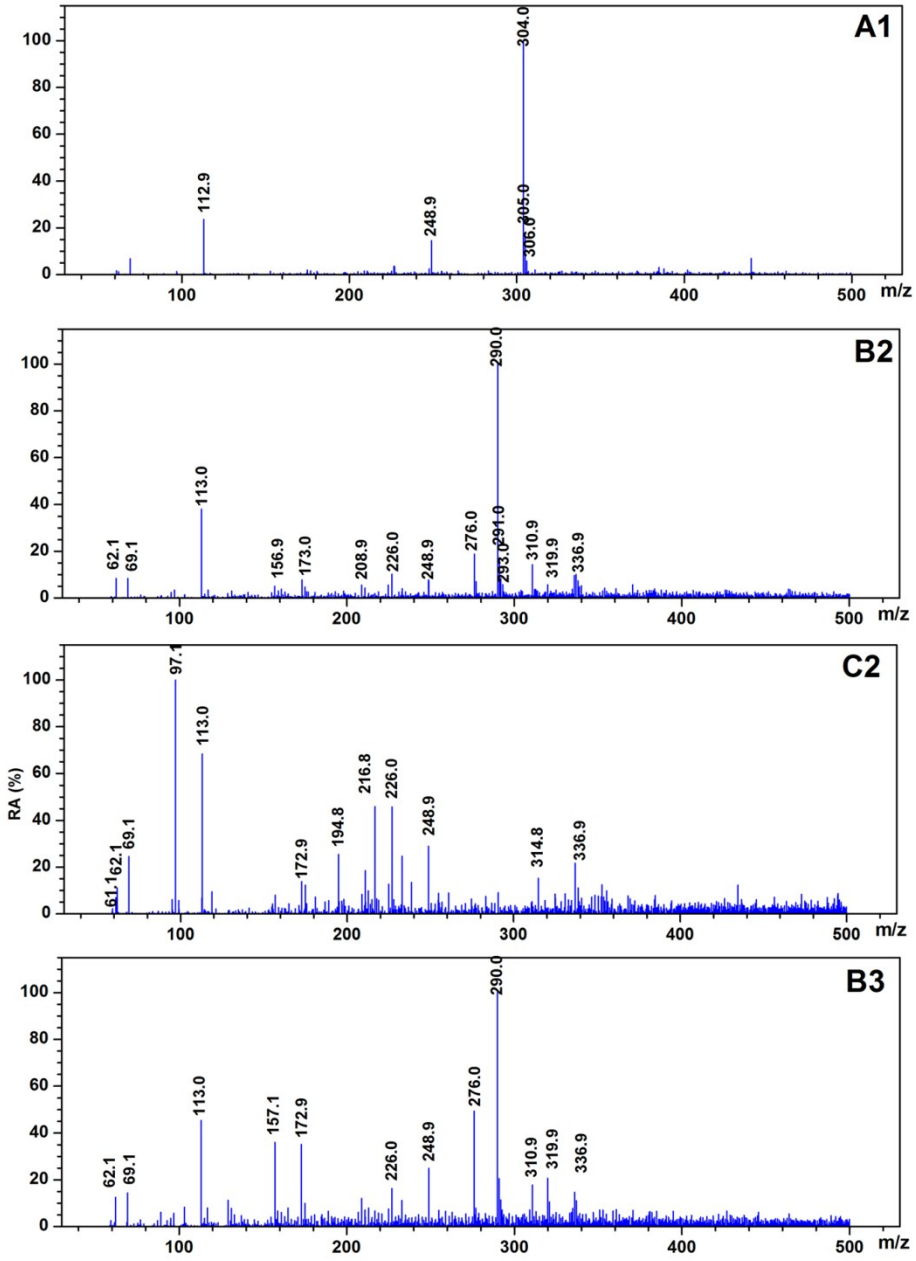

Fig. S7: Negative ion ESI mass spectra in the photodegradation of MO intermediate products. Spectra labelled (A1, B2, C2, and B3) represent peaks as shown in Fig. S6.

Fig. S8 [Patra *et al*]

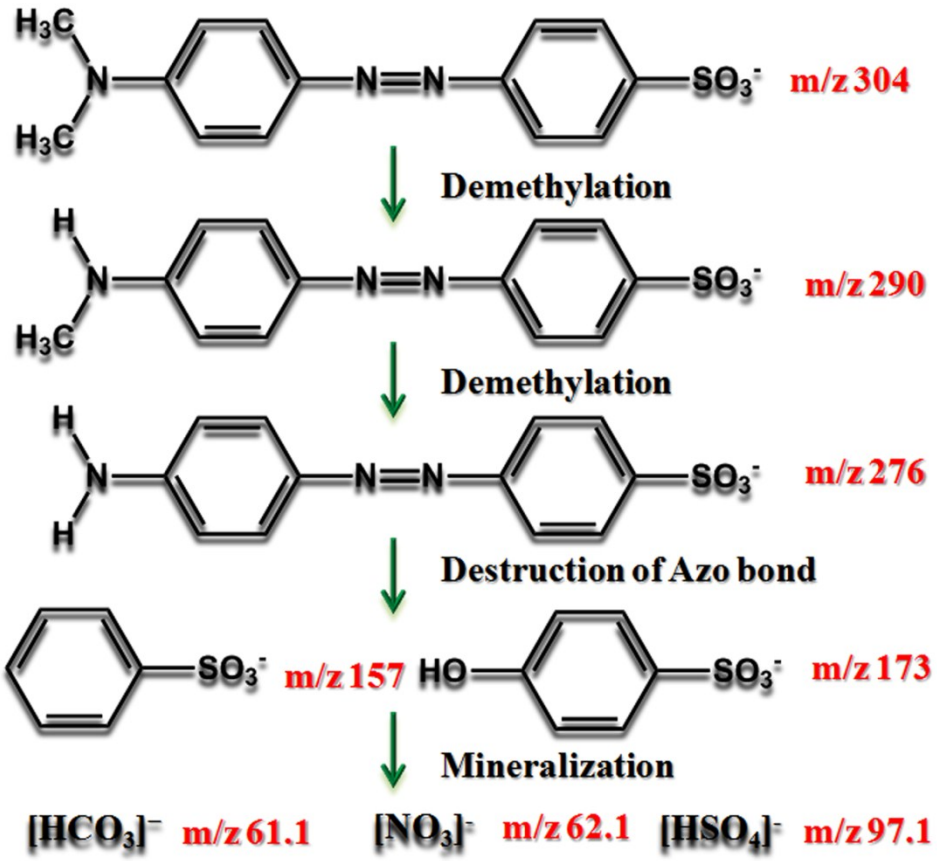

Fig. S8: The proposed mechanism of MO degradation.

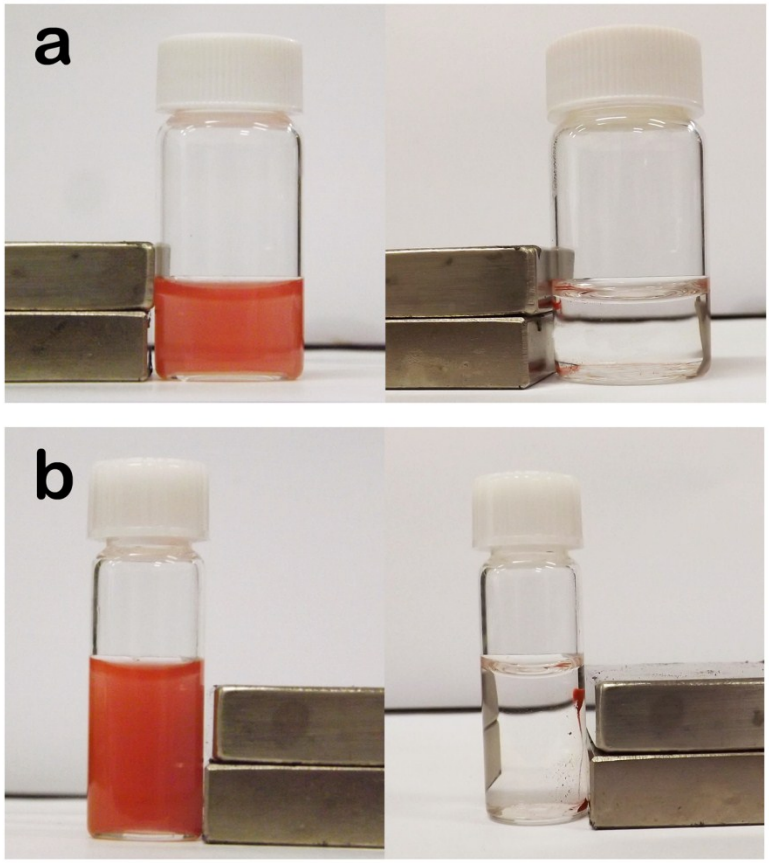

Fig. S9. Photograph of nanocatalyst in the reaction mixture (left), and after the reaction, nanocatalyst was separated from the reaction solution by using an external magnet (Right). (a) Bitruncated-dodecahedron, (b) Bitruncated-octahedron shape hematite

Fig. S10 [Patra *et al*]

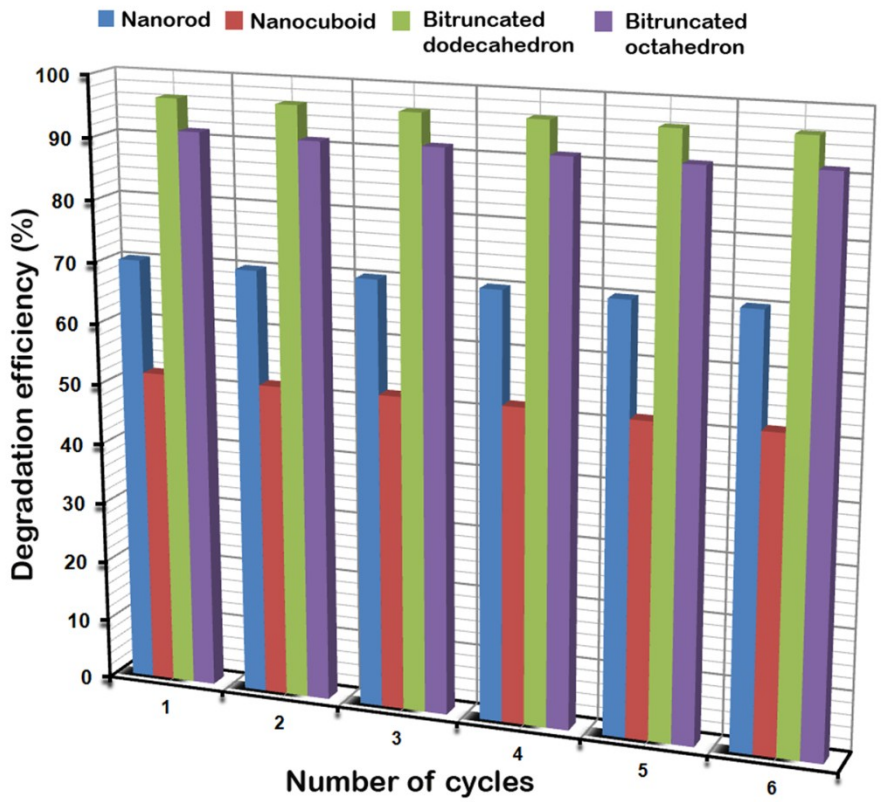

Fig. S10: Recycling efficiency of facets-driven hematite nanocrystals with different crystal facets for the MO degradation in visible light irradiation; duration of each runs spanning 3 hrs.